AAS 08-052

RADIOMETRIC TRACKING FOR DEEP SPACE NAVIGATION

James S. Border, Gabor E. Lanyi, and Dong K. Shin

Jet Propulsion Laboratory, California Institute of Technology

31st ANNUAL AAS GUIDANCE AND CONTROL CONFERENCE

February 1-6, 2008
Breckenridge, Colorado

Sponsored by
Rocky Mountain Section

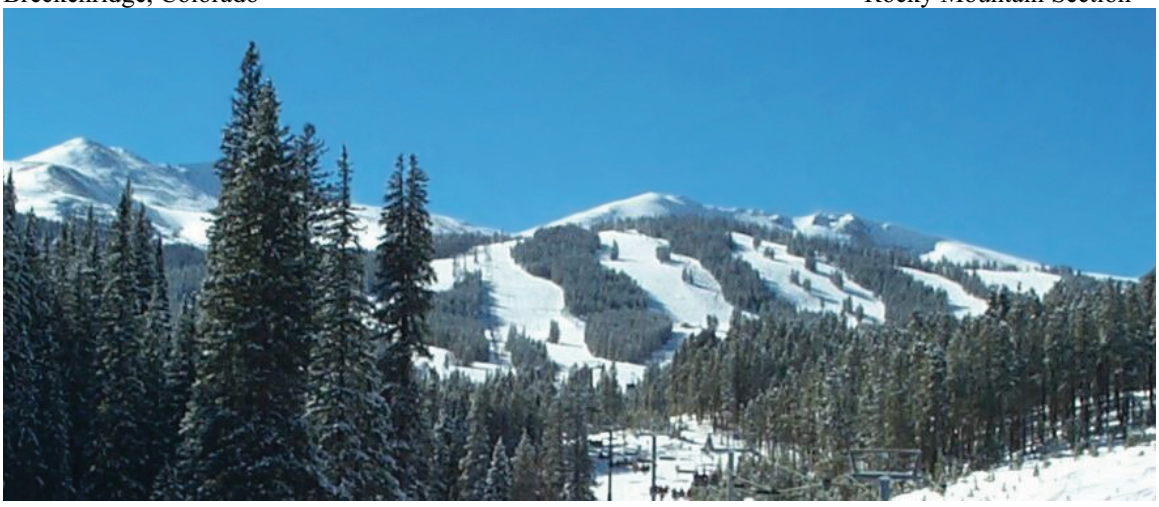

AAS Publications Office, P.O. Box 28130 - San Diego, California 92198

AAS 08-052

RADIOMETRIC TRACKING FOR DEEP SPACE NAVIGATION

James S. Border*, Gabor E. Lanyi#, and Dong K. Shin#

Metric information derived from radio communication links between Earth and spacecraft are used for navigation of interplanetary probes. This paper summarizes radiometric techniques and their error budgets. Measurements of the shift between transmitted and received frequency determine the line-of-sight velocity of the probe. In addition, measurements of the elapsed time between transmission of a pulse and its reception determine line-of-sight distance. Finally, measurements of the difference in arrival time of a spacecraft signal between two stations determine the angular spacecraft position. The Deep Space Network (DSN), with three tracking complexes spaced around the globe, provides communication links with all NASA interplanetary probes. Radiometric measurements as implemented in the DSN are described. Reference frame definition, tracking station coordinates, calibrations for the orientation of Earth, and calibrations for transmission media delays are also described. Error budgets are presented for all three data types that show the contributions of the various factors. Typical accuracies for DSN metric observables are 0.06 mm/sec for line-of-sight velocity, 75 cm for line-of-sight distance, and 2.5 nrad for angular position. Tracking measurement results from several recent missions are shown and compared to the error budgets. Limiting error sources are identified. In order to support navigation of more challenging missions planned for the future, possible improvements in radiometric tracking techniques are considered.

INTRODUCTION

Radio communication links between Earth and spacecraft have been used for navigation of interplanetary probes since the beginning of the space age. Measured properties of a radio signal convey information about the relative position and velocity of transmitters and receivers. When measurements of a spacecraft radio signal are made at a tracking station with known coordinates, information about the spacecraft position and velocity may be inferred. Measurements of the shift between transmitted and received frequency determine the line-of-sight velocity of the probe. Further, measurements of the elapsed time between transmission of a pulse and reception of the same pulse determine line-of-sight distance. Finally, measurements of the difference in arrival time of a spacecraft signal at two stations determine the angular spacecraft position. The Deep

* Principal Engineer, Tracking Systems and Applications Section, Jet Propulsion Laboratory, California Institute of Technology, 4800 Oak Grove Drive, Pasadena, California 91109, James.S.Border@jpl.nasa.gov

Senior Engineer, Tracking Systems and Applications Section, Jet Propulsion Laboratory, California Institute of Technology

Space Network (DSN), with three tracking complexes spaced around the globe, provides communication links with all NASA interplanetary probes and also supports some missions from other space agencies. The DSN has developed systems for making precise measurements of radio signals and forming observables that are used for spacecraft navigation. Frequency shift measurements are referred to as Doppler, measurements of signal propagation time between station and spacecraft are referred to as range, and difference in arrival time measurements at two stations are referred to as delta differential one-way range (ΔDOR).

Each of these three basic techniques was implemented in the DSN by the late 1970's[1]. Supporting media propagation and Earth orientation calibrations were also provided to enable proper interpretation of the data within the navigation process. Data are normally acquired during every communications contact, which may be as often as daily or as sparse as weekly depending on the mission. One might wonder why so much data are required, since spacecraft generally travel along conic sections which can be defined by three points. However, there are two complicating factors. First, orbits are perturbed by solar pressure, gas leaks, thruster firings, gravity fields, third body influence, etc. Second, the three dimensional state must be inferred from measurements that are barely more than one dimensional. Due to these factors most deep space navigation applications are forced to work with data sets that are somewhat incomplete. This can be contrasted with a GPS user on Earth. The GPS user gets three dimensional geometric coverage while the probe in deep space sees Earth as a point.

Continual improvements in data accuracy and calibration accuracy have occurred over the past three decades. While progress through the year 2000 is documented in Ref. 2, this paper reports on current system performance. Today, measurements are made at accuracies approaching limits set by the available spacecraft radio signal spectrum. The accuracy of the data depend on a number of factors including signal strength, signal structure, and observing geometry. Typical metric accuracies for DSN observables are 0.06 mm/sec for line-of-sight velocity, 75 cm for line-of-sight distance, and 2.5 nrad for angular position. In the following sections of this paper, the three types of radiometric measurements are described in more detail. Associated calibrations are discussed. Error budgets are presented for all three data types that show the contributions of the various factors. Tracking measurement results from several recent missions are shown and compared to the error budgets. Limiting error sources are identified. In order to support navigation of more challenging missions planned for the future, possible improvements in radiometric tracking techniques are considered.

DATA TYPES

Several alternative types of measurements are used for spacecraft navigation depending on mission requirements. Earth-based radiometric tracking is used throughout cruise and often during final approach and orbit insertion. On-board measurements such as optical images or radar may be needed to locate a target with a poorly known

ephemeris. Proximity links may be used for relative navigation between assets such as rovers and orbiters at another planet. Guidance during atmospheric descent may require landmark tracking. Selecting capabilities and the data mix needed for navigation is part of mission design. This paper focuses on Earth-based radiometric tracking. Complete definitions of radiometric data types are given by Moyer[3]. Conceptual definitions of radiometric data types are given in this section. Actual implementation of the radiometric measurement system in the DSN differs in detail from the description given here, but provides equivalent observables.

Doppler

Doppler is a phase delay measurement derived from a narrowband carrier signal using a phase-locked loop. The carrier is reconstructed in the case of suppressed carrier transmission. During acquisition, the received spacecraft signal is mixed with a reference signal tied to the station frequency standard. The beat note is then measured, as shown in Figure 1. Two-way data (signal transmitted by station; coherently transponded by spacecraft; received at station) provide the best accuracy today due to the high stability of the station frequency standard. One-way data (signal transmitted by spacecraft; received at station) are strongly affected by frequency drift and offset between spacecraft and station clocks. Precision at the mm-level or better is obtained from microwave frequencies (S, X, or Ka band) for range change. Absolute phase cannot be measured, but rather phase change over time is the observed quantity.

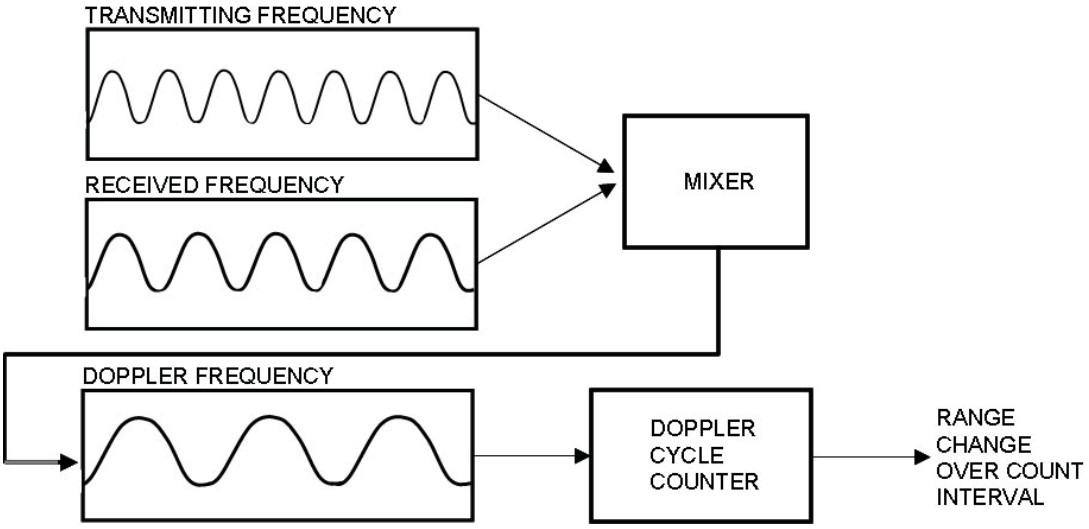

Figure 1 Doppler Extraction Process

As an example, consider a typical situation where the Doppler reference frequency is the same as the transmitter frequency. The received phase $\phi(t)$ (in units of cycles) is related to the transmitter frequency f_T (Hz) and the round-trip range $\rho(t)$ (s) by

$$\phi(t) = f_T\left(t - \rho(t) - t_0\right) \tag{1}$$

The Doppler observable over the measurement interval t_s to t_e is given by

$$f_T - \frac{\phi(t_e) - \phi(t_s)}{t_e - t_s} = f_T \frac{\rho(t_e) - \rho(t_s)}{t_e - t_s} \tag{2}$$

The left hand side of Eq. (2) is the observed Doppler and can be viewed as the transmit frequency minus the receive frequency. The right hand side is the physical quantity being measured. The navigation process develops model values of the trajectory and other parameters to fit the data. High precision is obtained even from a relatively weak signal. If the received carrier power to noise spectral density is 10 dB•Hz, then, with 1-sec phase measurement integration and a 60-sec measurement interval, the one-way range-rate precision is 0.015 mm/s. Space loss scales as $1/R^2$ where R is the station-spacecraft distance. Note that to obtain one-way range-rate in units of mm/s, Eq. (2) should be multiplied by the radio frequency wavelength (mm/cycle) and then divided by two.

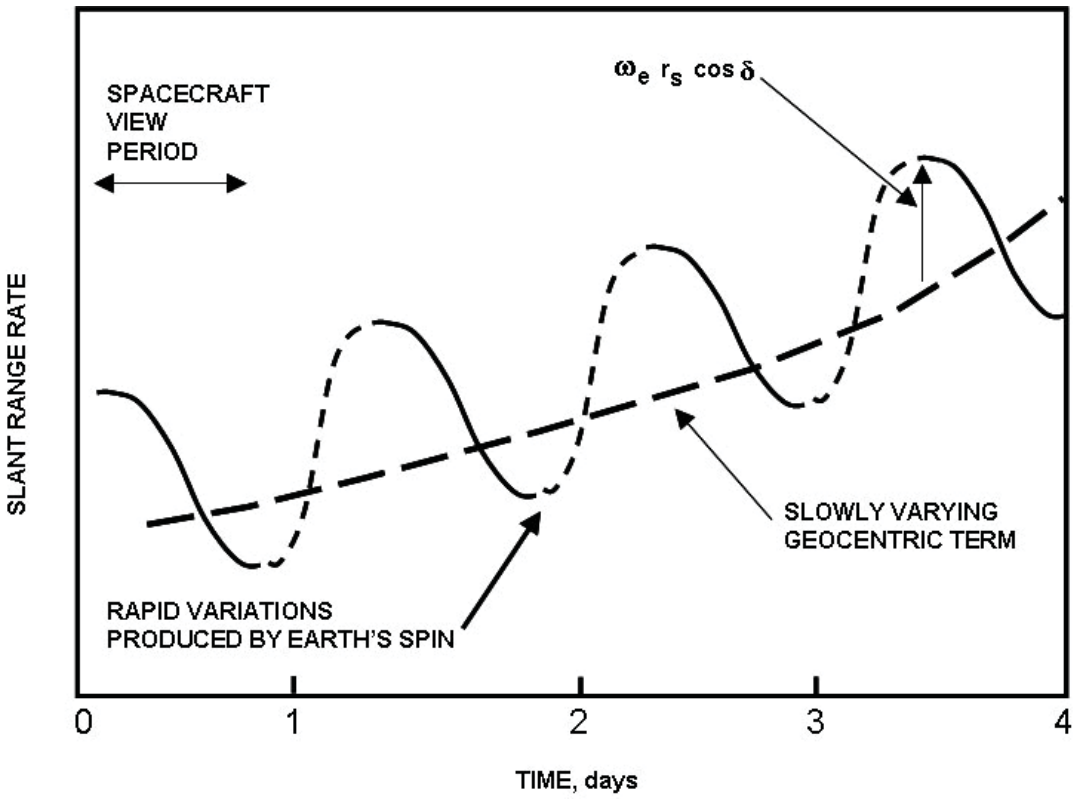

Figure 2 Information Content in Diurnal Doppler Signature

Doppler is the most versatile of all radiometric data types. It is collected during most times when there is radio communication between Earth and spacecraft. It is used to monitor small motions of the spacecraft including attitude changes, rotation, and small accelerations. It is used to calibrate on-board thrusters and to determine solar pressure reflection coefficients. Doppler directly provides one component of state, namely line-of-sight range-rate. These data are used to monitor one component of velocity. Realtime

displays of measured versus predicted Doppler are especially useful during critical events. Further, an arc of data (4 to 8 hr) is sensitive to spacecraft geocentric right ascension and declination through geometry changes due to Earth rotation. The information content in Doppler data is shown in Figure 2.

Range

Range is a group delay measurement derived from codes (either sinusoidal tones or pseudonoise (PN) codes) modulated on the spacecraft carrier signal. During processing at the ground station, the ranging signal is demodulated from the received spacecraft signal and correlated with a model ranging code tied to the station frequency standard. The phase offset between the received code and the model code is measured. This phase offset depends on the elapsed time between signal transmission and signal reception. Two-way data (range code modulated on station uplink signal; code demodulated at spacecraft and re-modulated on downlink; signal transmitted to station) provide the best accuracy today due to elimination of clock offsets. One-way data are strongly affected by the epoch offset between spacecraft and station clocks. Precision at the m-level is obtained using a 1-MHz ranging code bandwidth and a few minutes of integration time. Absolute range is measured, but path delays through station and spacecraft electronics must be calibrated.

As an example, consider a range code that is a sine wave with frequency f_r. The model range code phase $\phi_r(t)$ is given by

$$\phi_r(t) = f_r(t - t_0) \tag{3}$$

The received range code phase at time t is equal to the value of the model phase at a light-propagation time earlier and the range correlator produces the code phase difference

$$\Delta\phi_r(t) = \phi_r(t) - \phi_r(t - \rho(t)) \tag{4}$$

The observed range is given by

$$\mathrm{R}(t) = \frac{\Delta\phi_r(t)}{f_r} + \frac{N}{f_r} \tag{5}$$

The integer N must be determined from a priori knowledge of the range. Normally, codes at lower frequencies are cycled through to successively resolve the ambiguity. Substituting for $\Delta\phi_r$, the observed range is shown to have the value

$$\mathrm{R}(t) = \rho(t) \tag{6}$$

Most missions flying today have a transponder that does not detect the uplink ranging signal, but rather turns around a nominal bandwidth consisting of both signal and noise. This is referred to as transparent ranging and results in ranging signals being weak in most cases. For the downlink, the spacecraft transponder ranging channel uses a small modulation index so most power may go to telemetry. It can be shown[4] that space loss goes as $1/R^4$ for the typical deep space weak signal case. For a typical case with a 1-MHz range code, a received range signal to noise spectral density ratio of P_R/N_0=0 dB•Hz, and 10 min integration time, the one-way range precision is 0.7 m. Note that to obtain one-

way range in units of cm, Eq. (6) should be multiplied by the speed of light (cm/s) and then divided by two.

Range data directly provide one component of state and are an important complement to Doppler data for navigation. A data arc of a few days provides sensitivity to ecliptic longitude through the signature introduced by the Earth's orbital motion. Further, ranging from both northern and southern hemisphere stations provides sensitivity to ecliptic latitude. Though range may be acquired continuously while Doppler are being acquired, at the present accuracy levels, the information content within a single pass is nearly one dimensional. If range precision were high enough, then range could serve as a substitute for most navigational applications of Doppler.

Delta-DOR

Differential one-way range (DOR) is a group delay measurement derived from a signal, typically a sinusoidal tone, modulated on the carrier. The spacecraft signal is received at two widely separated stations and the difference in time of arrival is measured. A DOR measurement must be calibrated with a similar VLBI measurement of a natural radio source to obtain useful accuracy. The spacecraft minus quasar delay measurement is referred to as ΔDOR. Unlike Doppler or range, one-way downlinks are normally used for ΔDOR measurements. Two-way measurements are not necessary since station differencing eliminates spacecraft clock errors while spacecraft-quasar differencing eliminates ground station clock errors. The ΔDOR observation geometry is illustrated in Figure 3. The vector between stations is referred to as the baseline. The observable for a single radio source is variously referred to as differential range or delay. Precision at the nrad-level is obtained using a DOR tone frequency of 19 MHz and an integration time of a few minutes.

As an example, consider a DOR tone that is a sine wave with frequency f_{DOR}. The received phase of the upper (+1st harmonic) DOR signal $\phi_{1u}(t)$ at station 1 is given by

$$\phi_{1U}(t) = (f_T + f_{DOR})(t - \rho_1(t) - t_0) \tag{7}$$

After differencing between upper and lower DOR harmonics and after differencing between ground stations, the double differenced phase is given by

$$\Delta\Delta\phi(t) = 2 f_{DOR}(\Delta\rho(t)) \tag{8}$$

The observed differential one-way range is given by

$$\text{DOR}(t) = \frac{\Delta\Delta\phi(t)}{2 f_{DOR}} + \frac{N}{2 f_{DOR}} \tag{9}$$

The integer N must be determined from a priori knowledge of the differential range. Tones or telemetry sidebands at lower frequencies are cycled through to successively resolve the ambiguity. The observed DOR is seen to have the value

$$\text{DOR}(t) = \Delta\rho(t) \tag{10}$$

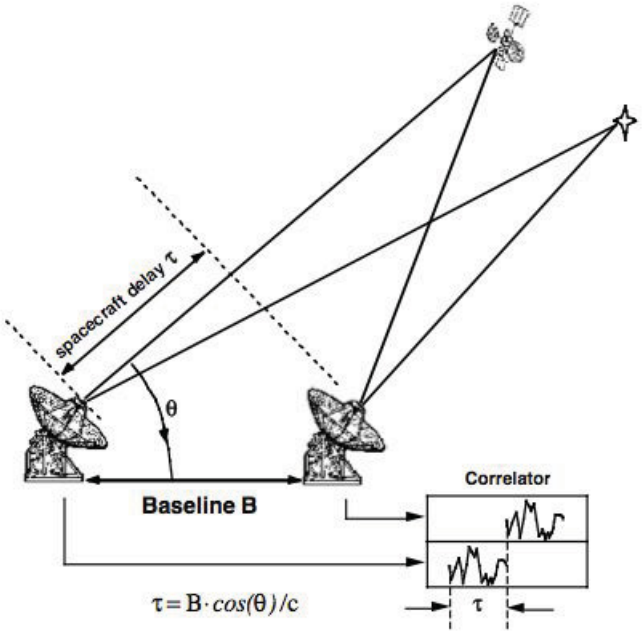

Figure 3 Delta-DOR Observation Geometry

For most missions, DOR tones are turned off except for a scheduled measurement interval. Spacecraft normally inhibit telemetry downlinks while a DOR measurement, including ground antenna slews to a quasar, is being made. For a typical case with a 19-MHz DOR tone, a received DOR tone to noise spectral density ratio of 20 dB•Hz, and 10 min integration time, the differential range precision is 0.024 ns. It should be noted that measurement precision and key systematic errors scale with $1/f_{DOR}$. Also, to convert Eq. (10) from delay (s) to angular position (rad), multiply the equation by the speed of light (km/s) and then divide by the baseline length (km). A value of 7200 km is used for unit conversions with DSN baselines.

A ΔDOR measurement provides an instantaneous value of spacecraft angular position. This is a geometric determination and is not dependent on dynamic force models. A precision of 0.024 ns over a 7200 km baseline gives an angular precision of 1 nrad. In turn, 1 nrad angular precision corresponds to 150 m in plane-of-sky spacecraft position at 1 AU distance. Data can only be acquired during the overlap period when the spacecraft is visible from both stations. Generally only a small number of measurements are made per day and per baseline. ΔDOR measurements on two baselines are needed to determine both components of angular position. The DSN baselines Goldstone/Madrid and Goldstone/Canberra are used for this purpose.

CALIBRATIONS

Precise observations of radio signals as described in the previous section must be modeled and calibrated in the navigation process. To describe signal propagation, models are needed for (i) the geometric position and motion of the tracking stations and the spacecraft, (ii) lighttime geodesics, (iii) instrumental delays, and (iv) delays introduced by media. While the state-of-the-art in these areas was maturing over a decade ago[2], the better data and modeling techniques available today from astrometric, geodetic, and satellite systems have led to improvements in accuracy.

Both a celestial reference frame for integrating spacecraft equations of motion and a terrestrial reference frame for defining tracking station coordinates are used during data reduction. The celestial reference frame is defined by the coordinates of quasars in the ICRF[5]. Spacecraft angular position is directly tied to this reference frame through the quasar coordinates used in ΔDOR data reduction. Observations of GPS satellites provide calibrations for tropospheric[6] and ionospheric[7] delays. VLBI observations combined with GPS observations provide Earth orientation calibrations[8] to tie the celestial and terrestrial reference frames together.

Sensitivity analyses of the dependence of navigation parameters on calibration parameters, combined with experience from many missions, have led to a good understanding of the relative importance and required accuracy of various calibrations. DSN systems have been implemented to meet both data and calibration accuracy requirements. A roadmap[9] has been developed to identify data and calibration accuracy requirements to meet the needs of current and anticipated future missions.

ERROR BUDGETS

While the formal error associated with a parameter estimate may scale down as the number of measurements increase, or as the data arc length increases, systematic effects due to instrumentation, media, force models, and uncertainty in geometric model parameters cause systematic effects at various time scales. These systematic effects typically dominate the magnitude of realistic error ellipses for spacecraft orbit determination. Proper characterization of systematic effects in radiometric data, and explicit modeling of these effects in the navigation process, are important in most problems of precision orbit determination.

In this section, error budgets are presented for the three radiometric data types. The contribution of each major effect, for a typical measurement scenario, is shown. Conditions and the size of error contributions may vary widely over the course of a mission, from launch to target arrival. The typical scenarios used in the error budgets are representative of conditions for the late cruise phase before arrival at target. The derivation of the error estimates presented here is beyond the scope of this paper, but may be constructed from the references.

The assumptions that have been used to generate the error budgets are shown in Table 1. These assumptions represent current capabilities in the Deep Space Network. The radio link is an X-band uplink and an X-band downlink. All uncertainties in Table 1, and in the error budgets to follow, are given at the one-sigma level. Metric uncertainties for Doppler and range are given for one-way range-rate and one-way range, respectively.

Table 1
ERROR BUDGET ASSUMPTIONS

Error Budget Component	One-Sigma Uncertainty
Solar Plasma	Based on measurements[10,11,12]
Tropospheric Scintillation	Based on measurements[10]
Zenith Troposphere Delay	1 cm
Line-of-Sight Ionosphere Delay	2.5 cm
Earth Orientation	3 cm
Station Location	2 cm
Quasar Coordinate	0.8 nrad

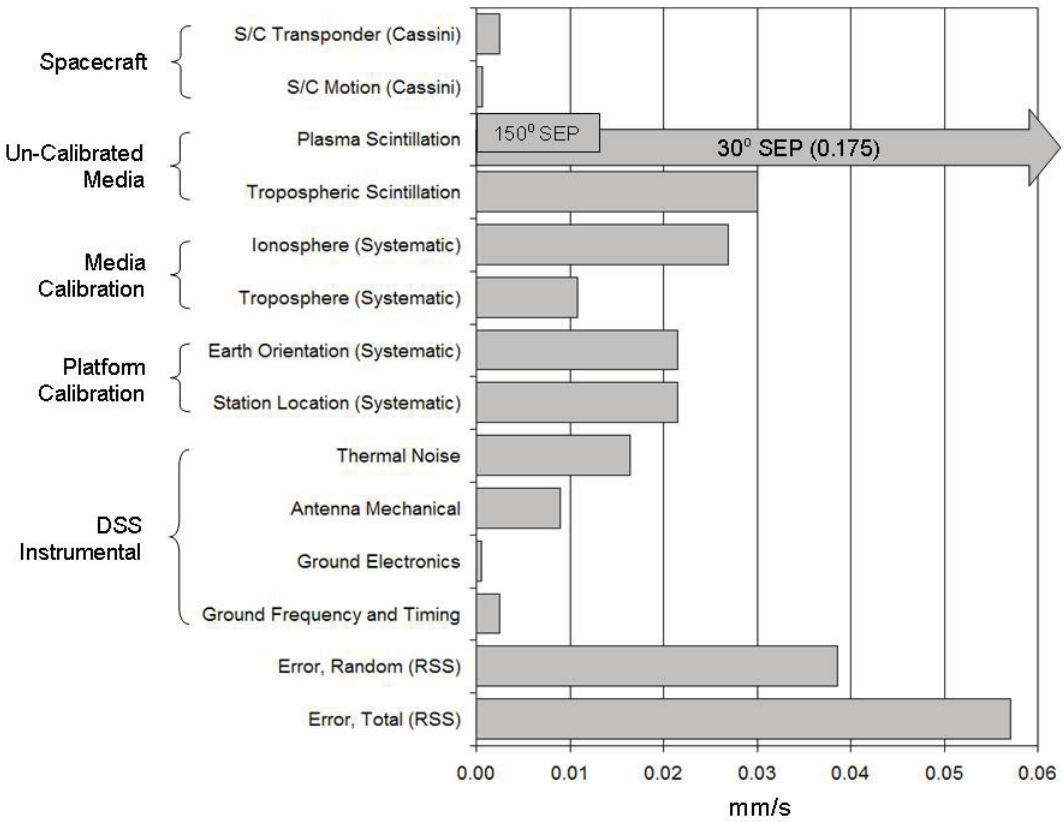

Figure 4 Deep Space Network Doppler Error Budget

Figure 4 shows an error budget for Doppler measurements. Effects that are labeled (Systematic) are intended to be modeled as explicit parameters in the navigation solution. All other effects are grouped together as a random error to associate with each data point. This error chart has been scaled to a 60 s measurement interval. Normally the random errors are treated as independent from one measurement to the next, though colored noise models may also be used if necessary to derive better statistics for certain orbit determination problems. The error contributions shown in the chart are not just the direct effect that a component might have on an instantaneous 60 s range-rate measurement, but rather the equivalent random noise corresponding to the uncertainty in that component. This has been done since the spacecraft orbit estimation process depends primarily on the signature in accumulated range change over a data arc. The equivalent noise has been determined by performing a sensitivity analysis for each component using a correct systematic model, and then comparing the estimated uncertainty in spacecraft right ascension with the uncertainty that would result from an independent random error. For example, realtime predictions for Earth orientation have an uncertainty of 2 cm in Earth rotation at the equator. Sensitivity analysis shows that this systematic effect will cause a spacecraft right ascension error of the same magnitude as that caused by a Doppler random error of 0.021 mm/s, for each 60 s interval, over an 8 hour data arc.

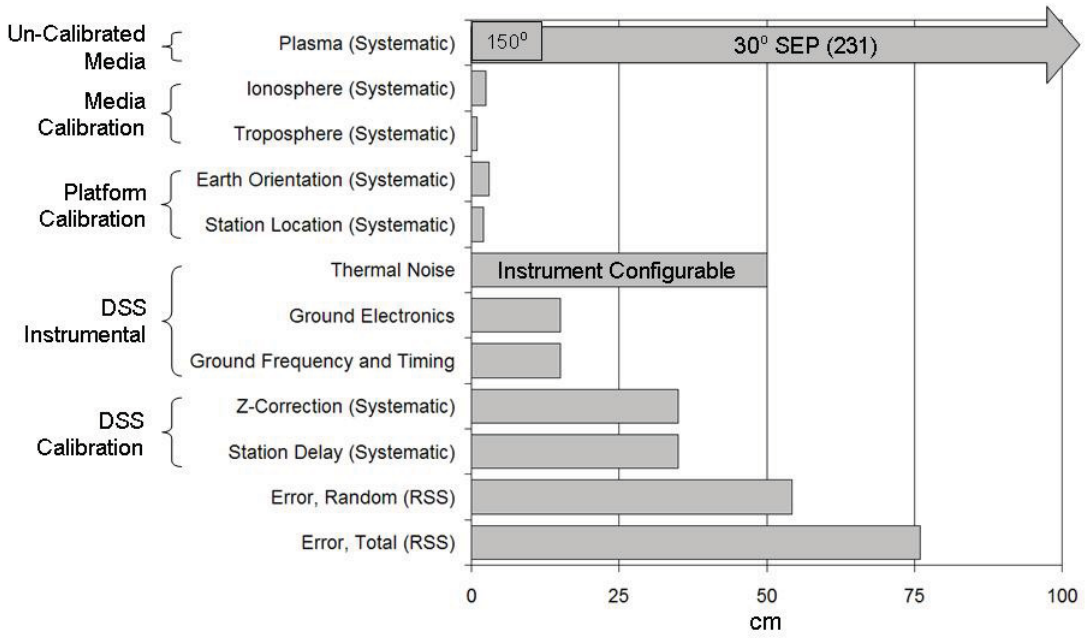

Figure 5 Deep Space Network Range Error Budget

In Figure 4, the components labeled 'Spacecraft' refer to unmodeled delay variations in spacecraft electronics and unmodeled spacecraft motion. Though these effects might not be considered an error in the measurement of the radio signal, they impact the interpretation of the Doppler observable. The components labeled 'Un-Calibrated Media' refer to short period media fluctuations that cannot be modeled or calibrated. The components labeled 'Media Calibration' and 'Platform Calibration' refer to effects that are modeled and calibrated. The errors shown in the chart are an estimate of the residual effects after calibration. The components labeled 'DSS Instrumental' refer to effects in the Deep Space Station (DSS) radio receiver system.

The solar plasma scintillation varies strongly with the Sun-Earth-Probe (SEP) angle. The value given for 150° SEP has been used to compute the root-sum-square (RSS) errors. The bar labeled 'Error, Random' does not include any components identified as (Systematic) in the charts, while the bar labeled 'Error, Total' includes all components. Similar conventions are used for the range error budget shown in Figure 5 and for the ΔDOR error budget shown in Figure 6.

The signal delay through the ground station microwave path and electronics must be calibrated for range measurements. Uncertainty in this calibration is often the dominant error for ranging and is referred to as a per station or per pass range bias. The delay is calibrated in two steps. A test signal is run through electronics common, as much as possible, to the path used for the spacecraft signal. The delay based on this measurement is labeled 'Station Delay' in Figure 5. The component labeled 'Z-Correction' refers to a combined measurement and calculation of the delay due to the test equipment, microwave optics not common to the test path, and an offset between the antenna phase center and antenna location reference point.

While ΔDOR is largely a self calibrating data type due to differencing of signals between stations and between spacecraft and quasar, the same effects that cause errors for Doppler and range also contribute residual errors to ΔDOR. The ΔDOR error budget shown in Figure 6 is balanced in the sense that errors due to most components are roughly of the same magnitude. For all three data types it is evident that improvements would need to made in at least several components to realize an overall improvement in accuracy. The typical root-sum-square errors for the three data types are summarized in Table 2. While precision improves with the number of measurements, components included as part of the total error, due to instrumentation, media, and uncertainty in geometric model parameters, cause systematic effects at various time scales.

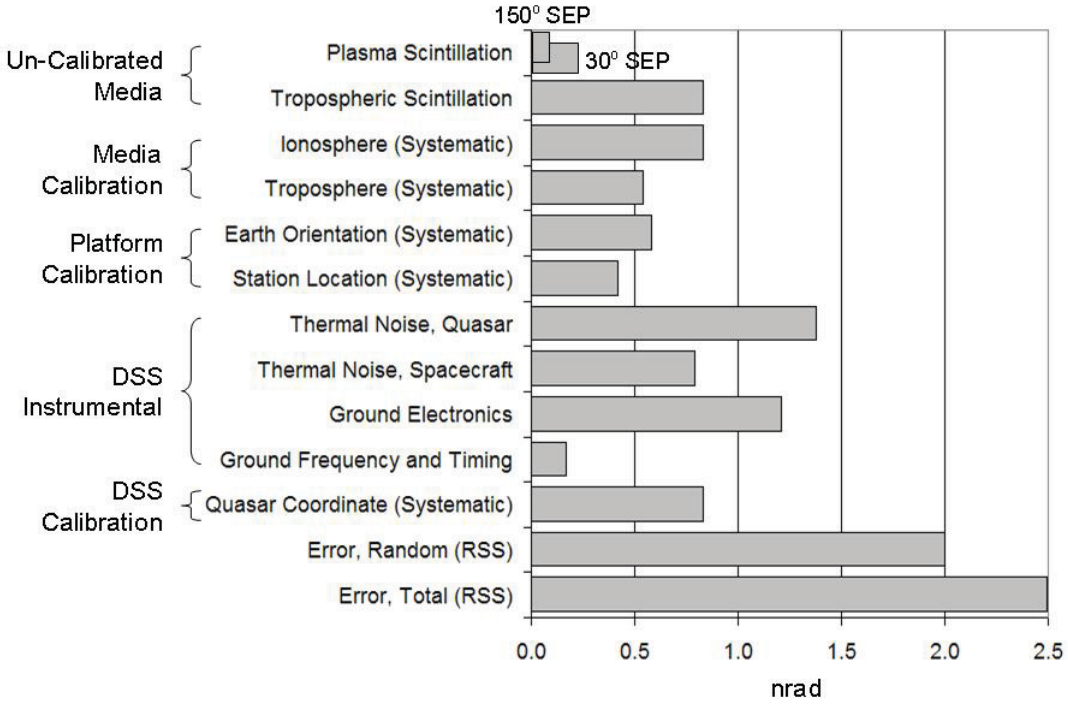

Figure 6 Deep Space Network ΔDOR Error Budget

Table 2
Typical Radiometric Data Accuracy (One-Sigma)

Data Type	Averaging Time	Random Error	Total Error
Doppler	60 sec	0.04 mm/s	0.06 mm/s
Range	600 sec	50 cm	75 cm
ΔDOR	600 sec	2.0 nrad	2.5 nrad

MEASUREMENT RESIDUALS

Development of error budgets for radiometric data is based on many things including theory and external characterizations of components of the measurement system. But analysis of data residuals has also played an important role in error budget development. Here we show plots of data residuals from several recent missions to compare to the predicted error budgets.

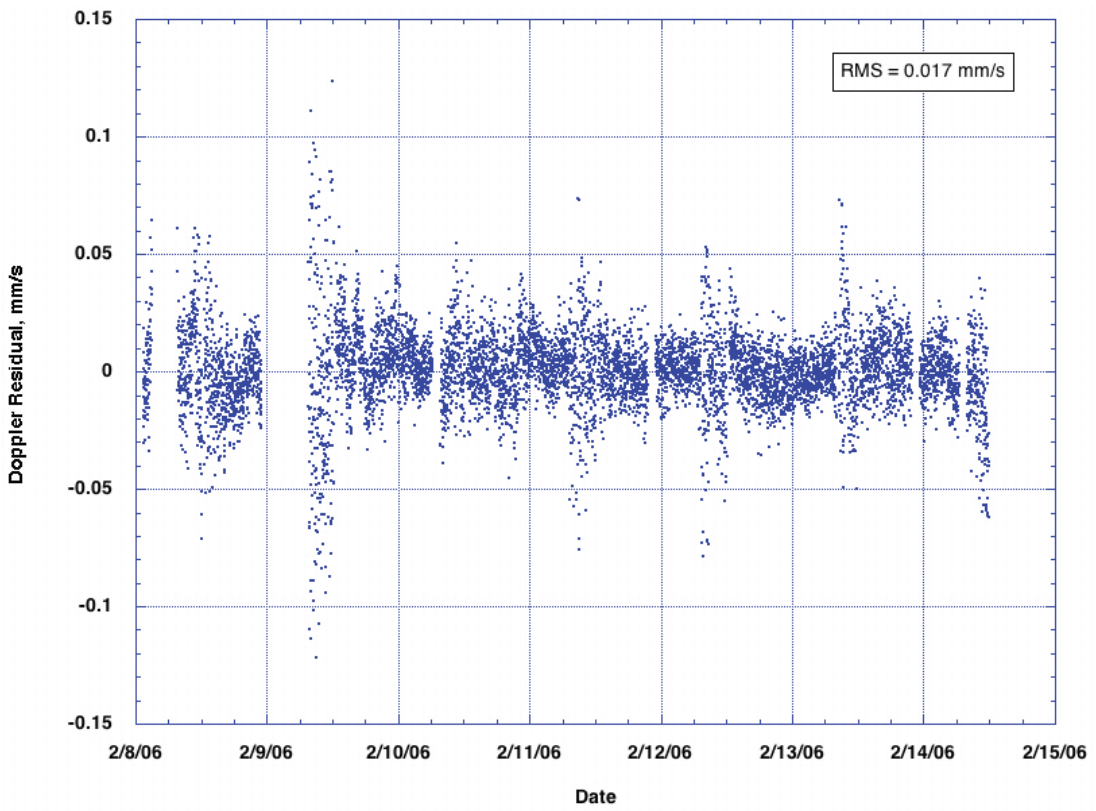

Figure 7 Mars Reconnaissance Orbiter Doppler Residuals

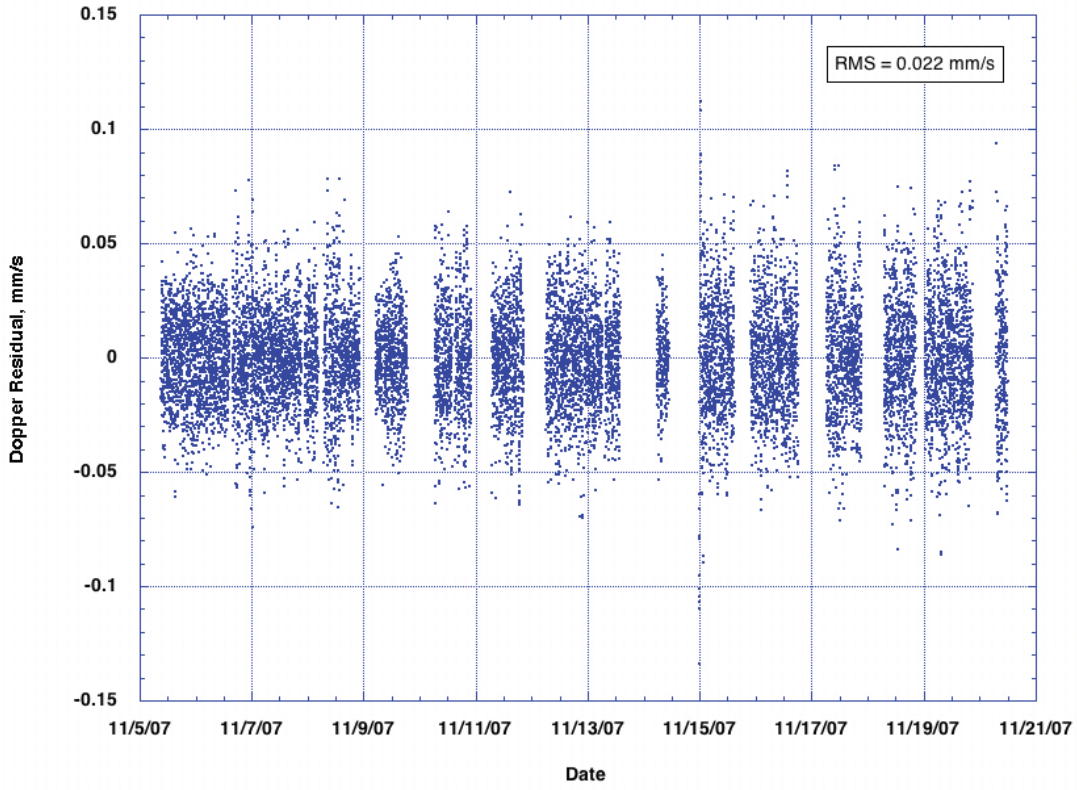

Figure 8 Phoenix Scout Lander Doppler Residuals

Doppler residuals from a one week period during the Mars Reconnaissance Orbiter (MRO) cruise phase are shown in Figure 7. MRO is about 165,000,000 km from Earth, along its journey toward Mars, and at a Sun-Earth-Probe angle of about 94 deg. Data from 21 different tracking passes over 8 different stations are shown. The root-mean-square (RMS) of the residuals is less than the quoted typical value in the error budget due to the strong signal and clean dynamics for this spacecraft. Tails due to media fluctuations may be seen near the beginning and end of most tracking passes, as the station elevation angle drops and the signal passes through more atmosphere. The low elevation data may be de-weighted or even deleted in the orbit determination process.

Doppler residuals from a two week period during the Phoenix cruise phase are shown in Figure 8. Phoenix is about 33,000,000 km from Earth, along its journey toward Mars, and at a Sun-Earth-Probe angle of about 131 deg. Though the tails in these data are similar to the tails seen in Figure 7, and the residual RMS is similar, the data for the central part of the tracking passes are about twice as noisy as the corresponding data in Figure 7. This is due to small unmodeled motions of the spacecraft caused by frequent jet firings to maintain attitude.

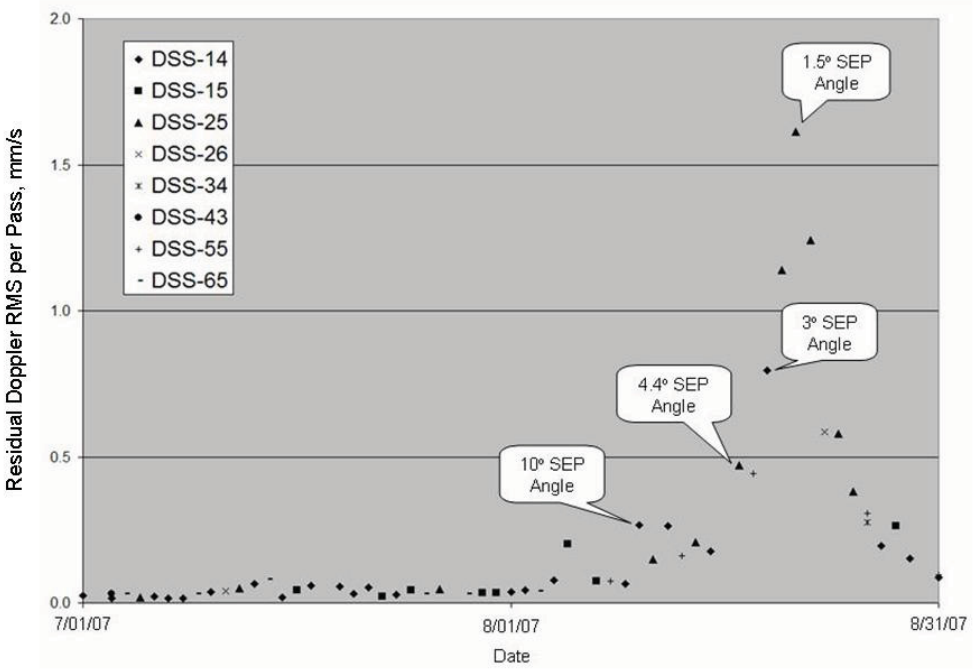

Figure 9 Cassini Doppler Residual RMS at Low Sun-Earth-Probe Angles

Doppler data are strongly affected by solar plasma fluctuations for raypaths that pass close to the Sun. Figure 9 shows the residual Doppler RMS over individual tracking

passes for the Cassini spacecraft during a two month interval including a solar conjunction. Cassini is in orbit about Saturn and about 1,530,000,000 km from Earth. The residual RMS grows to as large as 16 mm/s for Sun-Earth-Probe (SEP) angles less than 2 deg. Radiometric measurements become unreliable at X-band frequencies for SEP angles less than 1 deg.

Range residuals from a one week period during the Mars Reconnaissance Orbiter cruise phase are shown in Figure 10. These data are from the same times and stations as shown in Figure 7 for Doppler. Again, for MRO, the RMS of the residuals is less than the quoted typical value in the error budget. The strong spacecraft signal reduces the random error to a very small value for most passes. The error in the station delay calibrations is the most visible effect for this data span. Jumps in the residual value are clearly seen from one tracking pass to the next. The residual trends within a pass may be unmodeled spacecraft motion, electronic variations, or media variations.

Range residuals from a two week period during the Phoenix cruise phase are shown in Figure 10. These data are from the same times and stations as shown in Figure 8 for Doppler. For Phoenix, the random noise is larger due to use of a medium gain rather than high gain antenna on the spacecraft. The random noise within a pass is the most visible effect over this time span. The bias from one pass to the next, due to an error in station delay calibration, can also be seen.

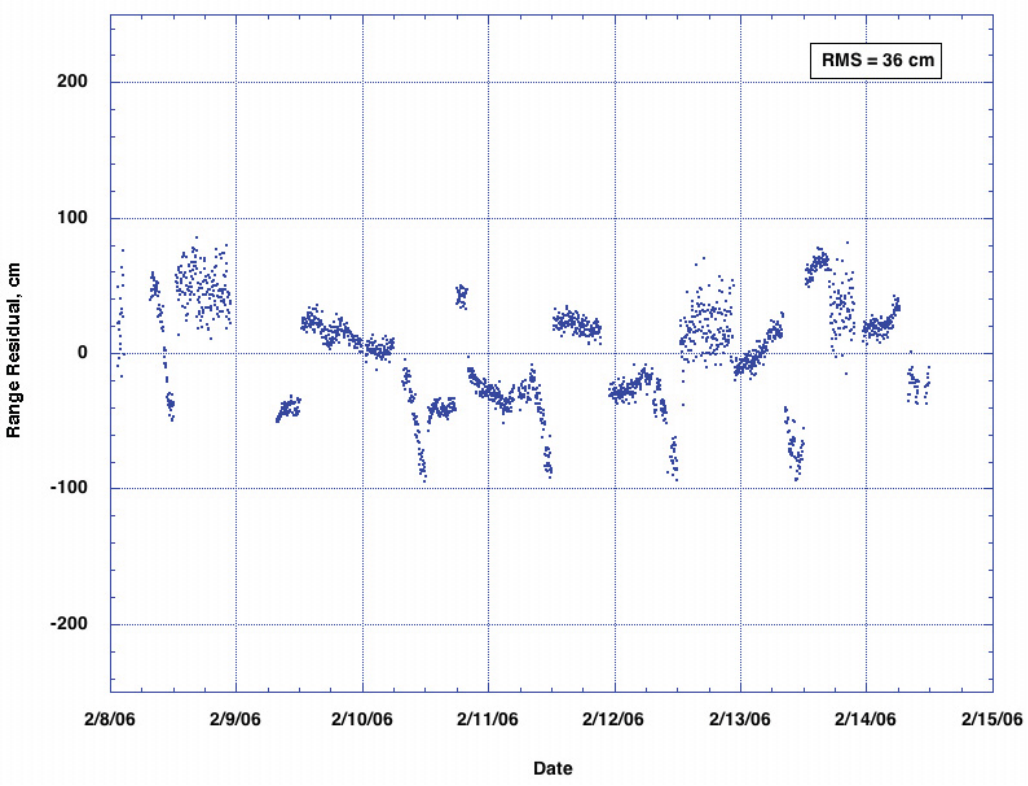

Figure 10 Mars Reconnaissance Orbiter Range Residuals

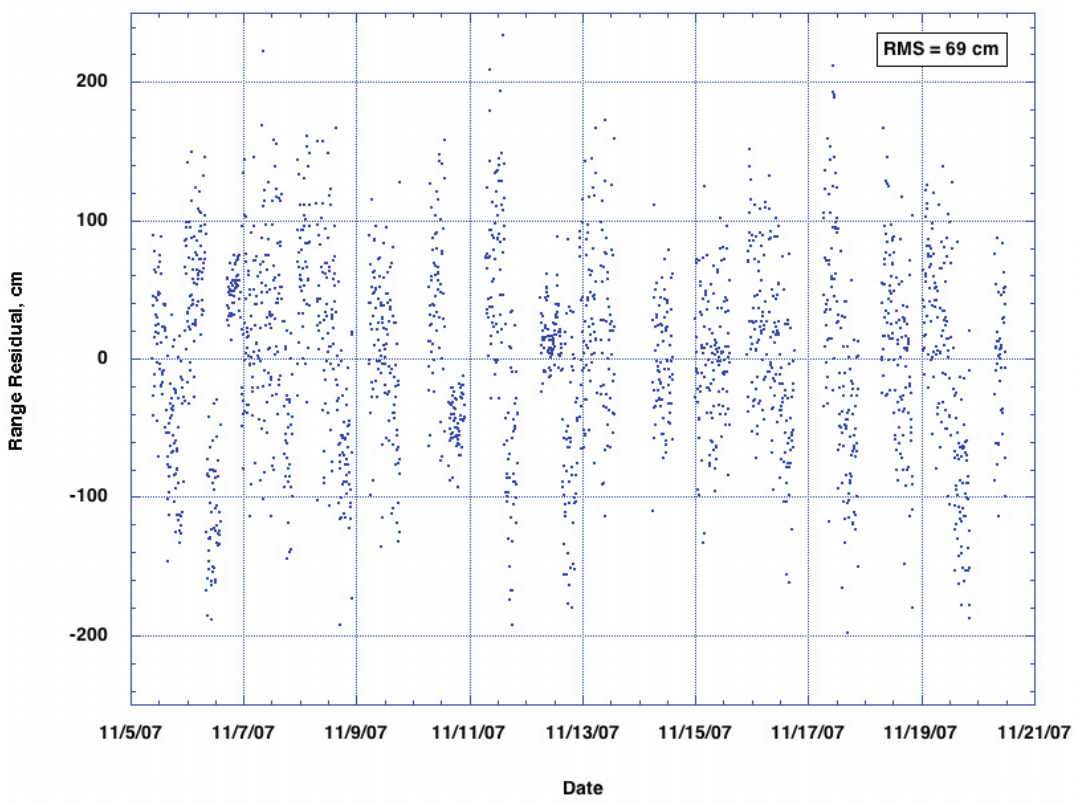

Figure 11 Phoenix Scout Lander Range Residuals

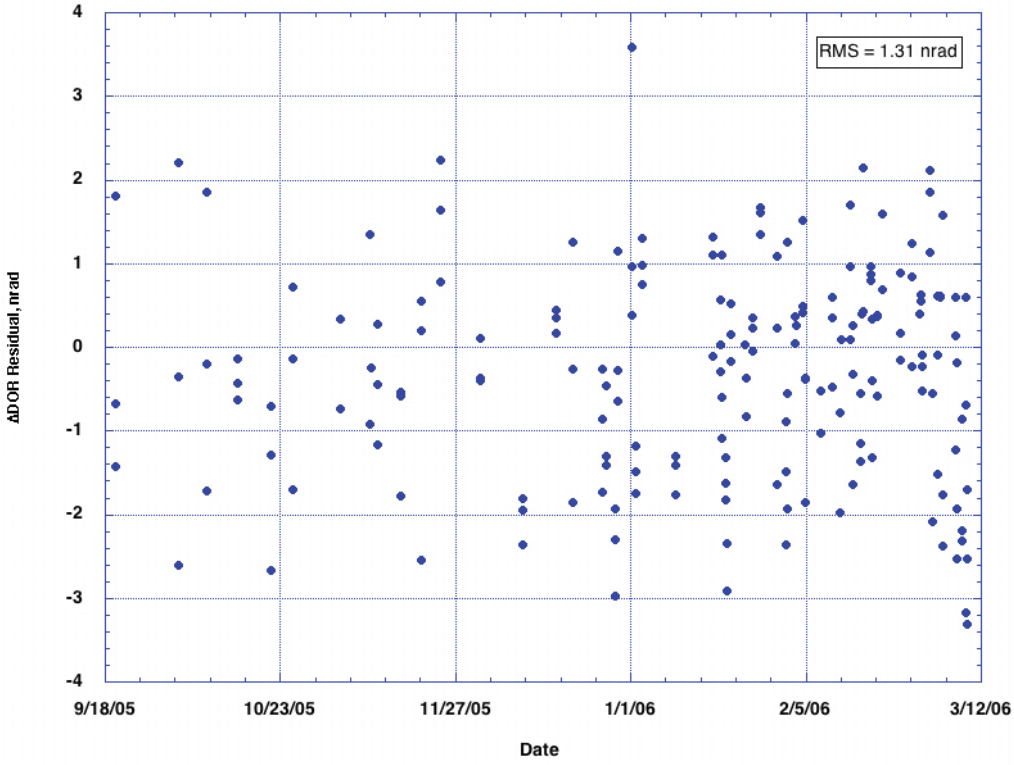

Figure 12 Mars Reconnaissance Orbiter ΔDOR Residuals

During MRO cruise phase, data were acquired during 64 ΔDOR sessions in support of navigation. Good performance is expected for MRO since the spacecraft is moving through the ecliptic plane with positive declination, viewing geometry is favorable from both DSN baselines, and a large number of reference radio sources is available. Nine radio source observations in three sequences of quasar1-spacecraft-quasar2 were made during each 1-hour session, generating three separate spacecraft minus quasar delta delay points. The measurement residuals to the final cruise trajectory are shown in Fig. 12. The RMS of residuals is 1.31 nrad, in good agreement with expected system performance. For all residual plots, the RMS could be a slight underestimate of true error since the spacecraft trajectory was fit to the data.

LIMITING ERROR SOURCES AND POTENTIAL IMPROVEMENTS

The error budgets presented here represent the measurement accuracy that the Deep Space Network can provide over a wide range of conditions corresponding to navigation tasks throughout the solar system. Measurement accuracy can be much better under special or favorable conditions. Also, science experiments conducted using spacecraft radio links may use additional resources to obtain better accuracy. The Cassini gravity wave experiment made use of a more elaborate radio system[10]. Signals were uplinked at both X-band and Ka-band. The spacecraft transponded the X-band uplink at both X-band and Ka-band. The Ka-band uplink was separately transponded at Ka-band. The use of these multiple frequency links enabled complete cancellation of errors due to solar plasma and ionosphere. In addition, a water vapor radiometer was used at the ground station to calibrate line-of-sight delay change due to water vapor fluctuations. Doppler accuracies better than 0.001 mm/s were achieved for a 1000-s interval.

Here we discuss the limiting error sources in measurements made for the purpose of navigation. Thermal noise is rarely a limiting factor since longer integration times effectively reduce this error term. Accuracy at short time scales is usually limited by media fluctuations. Errors due to solar plasma and ionosphere can be reduced by a factor of 15 by making use of Ka-band radio links instead of X-band. To realize this improvement for Doppler and range, both uplink and downlink must be at Ka-band. Ka-band for downlink only would provide this improvement for ΔDOR. Tropospheric scintillations can be reduced by a factor of 2 to 10 through the use of water vapor radiometers at the tracking stations to provide calibrations.

Systematic errors in tropospheric and ionospheric calibrations can limit accuracy for Doppler, at longer time scales, and for ΔDOR. Observations of GPS satellites from receivers located near the tracking stations are the primary source of data for these calibrations. The relative sparseness of the GPS constellation makes it difficult to map media delay measurements to the spacecraft line-of-sight. But the intended development of a similar European satellite navigation constellation will provide denser coverage in the sky and likely improvements of a factor of 2 or more in global calibration accuracy.

Errors in realtime predictions of the rotation of Earth about its axis can limit accuracy for Doppler, at longer time scales, and for ΔDOR. The difficulty at present has been latency in processing of VLBI measurements made for the purpose of Earth orientation determination. Data transfer capabilities over the internet have already been demonstrated and accuracy improvements of a factor of at least three are readily possible. It is just a matter of time before high speed electronic data transfer for VLBI is widely available.

Range data are strongly affected by uncertainty in the calibration of path delay through station electronics. This has proved a difficult problem to overcome, primarily due to the complexity of the tracking stations. But wider bandwidth pseudonoise ranging codes are anticipated for future use. The wider bandwidth will provide more precision and it is expected that progress will then be made on identifying limiting errors in the calibration technique. Also, spacecraft will re-generate the code on board and errors due to thermal noise will be greatly reduced. Further, this will enable ranging to be done in the far outer solar system or to spacecraft with only low gain antennas.

A significant improvement in ΔDOR measurement accuracy is probably not possible at X-band frequencies. The spectrum allocation available for deep space research is limited, restricting the allowed bandwidth for the group delay measurements. More importantly, the measurement accuracy is already approaching the uncertainty level caused by source structure in the quasar coordinates themselves. But both of these problems could be reduced by using Ka-band frequencies. The spectrum allocation is 10 times wider at Ka-band and research indicates that radio sources are more compact at the higher frequencies. An overall improvement of a factor of 5 may be possible for ΔDOR measurements.

One-way measurements of Doppler and range are not competitive today with two-way measurements, but the development of highly stable clocks for flight could enable similar performance for one-way as for two-way data.

CONCLUSION

Radio communication links with spacecraft traversing the solar system provide essential information to support navigation. A large amount of data is typically needed since Earth-spacecraft geometry is nearly one dimensional. However, line-of-sight and plane-of-sky data types together provide full three dimensional coverage and robust trajectory solutions. The spacecraft telecommunication system design must provide for signal capabilities as called for in the mission plan. Navigation performance depends on signal strength, structure, stability, bandwidth, and availability. Factors affecting measurement accuracy are well known. For data that have been and are being acquired from many spacecraft, measurement residuals are generally consistent with error budgets tailored to the geometry and characteristics of specific data arcs. A significant improvement in radiometric measurement accuracy has been realized over the last decade. Limiting errors for existing measurement techniques are understood and

methods to further improve measurement accuracy have been identified. Radiometric measurements are expected to play an important role in navigation for most interplanetary missions well into the future.

ACKNOWLEDGMENT

We would like to thank Mark Ryne for providing Doppler and range residuals to the Phoenix trajectory and Eric Graat for providing Doppler, range, and ΔDOR residuals to the Mars Reconnaissance Orbiter trajectory.

This research was carried out at the Jet Propulsion Laboratory, California Institute of Technology, under a contract with the National Aeronautics and Space Administration.

REFERENCES

1. N. A. Renzetti, J. F. Jordan, A. L. Berman, J. A. Wackley, and T. P. Yunck, "The Deep Space Network – An Instrument for Radio Navigation of Deep Space Probes," JPL Publication 82-102, Jet Propulsion Laboratory, Pasadena, California, December 15, 1982.

2. C. L. Thornton and J. S. Border, Radiometric Tracking Techniques for Deep-Space Navigation, JPL Deep Space Communications and Navigation Series, Hoboken, New Jersey: Wiley, 2003.

3. T. D. Moyer, Formulation for Observed and Computed Values of Deep Space Network Data Types for Navigation, JPL Deep Space Communications and Navigation Series, Hoboken, New Jersey: Wiley, 2003.

4. J. B. Berner, S. H. Bryant, and P. W. Kinman, "Range Measurement as Practiced in the Deep Space Network," *Proceedings of the IEEE*, vol. 95, no. 11, pp. 2202-2214, November 2007.

5. A. L. Fey, C. Ma, E. F. Arias, P. Charlot, M. Feissel-Vernier, A.-M. Contier, C. S. Jacobs, J. Li, and D. S. MacMillan, "The Second Extension of the International Celestial Reference Frame: ICRF-Ext.2," *The Astronomical Journal*, vol. 127, no. 6, pp. 3587-3608, June 2004.

6. Y. E. Bar-Sever, C. S. Jacobs, S. Keihm, G. E. Lanyi, C. J. Naudet, H. W. Rosenberger, T. F. Runge, A. B. Tanner, and Y. Vigue-Rodi, "Atmospheric Media

Calibration for the Deep Space Network," *Proceedings of the IEEE*, vol. 95, no. 11, pp. 2180--2192, November 2007.

7. A. J. Mannucci, B. D. Wilson, D. N. Yuan, C. H. Ho, U. J. Lindqwister, T. F. Runge, "A Global Mapping Technique for GPS-Derived Ionospheric Total Electron Content Measurements," *Radio Science*, vol. 33, no. 3, pp. 565-582, May-June 1998.

8. R. S. Gross, "Earth Rotation Variations — Long Period," in *Physical Geodesy*, edited by T. A. Herring, Treatise on Geophysics vol. 11, Amsterdam, The Netherlands: Elsevier, 2007.

9. Tomas J. Martin-Mur, Douglas S. Abraham, David Berry, Shyam Bhaskaran, Robert J. Cesarone and Lincoln J. Wood, "The JPL Roadmap for Deep Space Navigation," AAS 06-223, Proceedings of the AAS/AIAA 2006 Space Flight Mechanics Meeting, Advances in the Astronautical Sciences, Volume 124, Pages 1925-1932.

10. S. W. Asmar, J. W. Armstrong, L. Iess, P. Tortora, "Spacecraft Doppler Tracking: Noise Budget and Accuracy Achievable in Precision Radio Science Observations," *Radio Science*, vol. 40, no. 2, RS2001, March 2005.

11. R. Woo and J. W. Armstrong, "Spacecraft Radio Scattering Observations of the Power Spectrum of Electron Density Fluctuations in the Solar Wind," *Journal of Geophysical Research*, vol. 84, no. A12, pp. 7288-7296, Dec. 1, 1979.

12. W. A. Coles and J. K. Harmon, "Propagation Observations of the Solar Wind Near the Sun," *The Astrophysical Journal*, vol. 337, no. 2, pp. 1023-1034, Feb. 15, 1989.